Applied Catalysis B: Environmental 192 (2016) 277–285

Contents lists available at ScienceDirect

Applied Catalysis B: Environmental

journal homepage: www.elsevier.com/locate/apcatb

Highly efficient photocatalysis toward tetracycline under simulated solar-light by Ag^+-CDs-Bi_2WO_6: Synergistic effects of silver ions and carbon dots

Zhuo Li, Lingyan Zhu*, Wei Wu, Shanfeng Wang, Liwen Qiang

Key Laboratory of Pollution Processes and Environmental Criteria, Ministry of Education, Tianjin Key Laboratory of Environmental Remediation and Pollution Control, College of Environmental Science and Engineering, Nankai University, Tianjin 300071, PR China

ARTICLE INFO

Article history:
Received 31 December 2015
Received in revised form 13 March 2016
Accepted 22 March 2016
Available online 1 April 2016

Keywords:
Bi_2WO_6
Carbon dots
Silver ions
Synergistic effects
Tetracycline

ABSTRACT

A novel Ag^+-carbon dots (CDs)-Bi_2WO_6 ternary composite with excellent solar-light-driven photocatalytic performance was firstly synthesized using hydrothermal-impregnation method. It was used to degrade tetracycline (TC) in water. 5Ag^+-CDs2.5-Bi_2WO_6 (0.5 g/L) displayed superior photocatalytic efficiency with nearly 100% removal of TC (20 mg/L) in 20 min and 64% mineralization in 90 min. The degradation reaction coefficient (k_{obs}) was approximately 1.8 times higher than pure Bi_2WO_6 as a result of the synergistic effects of Ag^+ and CDs co-doped on the surface of Bi_2WO_6. Both CDs and Ag^+ could effectively trap the photoexcited electrons generated by Bi_2WO_6, promoting the charge transfer and separation of electron-hole pairs. In addition, after accepting the electrons, Ag^+ was photoreduced to Ag attached to Bi_2WO_6 nanosheets. The plasmonic-Ag and CDs displayed stronger utilization of visible light capacities. Moreover, Ag^+ itself also served as an oxidant to degrade TC in water directly. Electron transfer mainly occurred in the order of $Bi_2WO_6 \rightarrow Ag \rightarrow CDs$. Superoxide radical species and photogenerated holes were predominant reactive species responsible for the photodegradation of TC. The study indicated that novel Ag^+-CDs-Bi_2WO_6 has a great potential for rapid and efficient treatment of organic pollutants in water.

1. Introduction

Contamination of organic pollutants in water has brought a challenge to sustainable environment and human health. Tetracycline (TC), the second most widely used antibiotic in the world, exhibits broad-spectrum antimicrobial activity against a variety of diseases and is often applied in human therapy and livestock industry [1,2]. Most of TC are excreted through feces and urine as unmodified parent compounds [3]. As a consequence, significant amount of TC has been detected in surface and potable water due to ineffective removal by conventional water treatment methods [4,5], and this situation becomes even worse due to misuse and abuse of TC.

Many advanced strategies, such as adsorption, ozonation, biodegradation, eletrocatalysis have been used to get rid of TC from water. Among them, photocatalysis employing semiconductor raises great attention due to its low cost, low toxicity, mild reaction conditions, and efficient mineralization [6–8]. TiO_2 is efficient in photocatalytic degradation of pollutants and has been commercialized. However, the application of TiO_2 is severely restricted by its wide band gap, which could only be excited by ultraviolet light less than 387.5 nm [9,10]. Bismuth-based oxides appear to be good candidates since most of them have a band gap in the visible range due to the interaction between 6s Bi and 2p O orbitals at the top of the valence band [11]. Bi_2WO_6 is one of the representative members of the aurivillius family and possesses desirable photocatalytic activity under visible-light irradiation [12]. Nevertheless, pure Bi_2WO_6 can only utilize limited area of spectrum, from ultraviolet to visible-light region shorter than 450 nm. The rapid recombination rate of its photoinduced electron-hole pairs also limits its application [13]. To address these problems, numerous studies were conducted on designing novel Bi_2WO_6-based photocatalysts.

Doping carbonaceous materials, such as C_{60}, active carbon, carbon nanotubes, graphene (oxide), and carbon nitride, is an effective approach to improve the chemical, optical and electronic properties of Bi_2WO_6. Carbon quantum dots, also known as carbon dots (CDs), is a new class of carbon nanomaterials with size below 10 nm.

* Corresponding author at: The College of Environmental Science and Engineering, Nankai University, Tongyan Road 38, Tianjin 300350, PR China.
E-mail address: zhuly@nankai.edu.cn (L. Zhu).

http://dx.doi.org/10.1016/j.apcatb.2016.03.045
0926-3373/

It attracts the interests of researchers because of its non-toxicity, biocompatibility, easy synthesis and chemical inertness. CDs have various structures, such as an amorphous nanocrystalline core with diamond-like carbon or graphitic carbon [14–17]. It can serve as photogenerated electron acceptors or donors. Besides, it can function not only as an efficient photocatalyst for highly selective oxidation, but also as a multifunctional component in photocatalyst design to promote wider spectrum absorption and separation of electron-hole pairs, as well as to stabilize semiconductors [18]. To date, CDs has been used to decorate some semiconductors such as TiO_2 [19], ZnO [20], Fe_2O_3 [21] to improve their performance in decolorization of dye in water.

Recently, several studies reported deposition of noble metal nanoparticles or ions (Au, Ag, Au^{3+}, Ag^+, Pt^{4+}) on TiO_2 to improve its photocatalytic activity [22–25]. Embedding noble metal ions or nanoparticles on Bi_2WO_6 could also construct metal-semiconductor heterojunction and significantly improve the photocatalytic performance [26–30]. It is generally recognized that Ag^+ in solution can be photoreduced to Ag and deposited on semiconductors under solar-light irradiation. Ag-plasmonic photocatalyst has been proved to exhibit enhanced photocatalytic activity in visible light regions [31,32]. However, the research about the hybrid of metal ions and CDs on Bi_2WO_6 is still limited.

The main objectives of current study were to fabricate a novel Ag^+-CDs-Bi_2WO_6 and investigate its performance of degrading TC in water under the irradiation of solar light. The important roles of CDs and Ag^+ as well as the mechanisms in this system were analyzed and discussed. Meanwhile, Ag^+-CDs-Bi_2WO_6 could be recycled as a ternary Ag-CDs-Bi_2WO_6 and still exhibited good photocatalytic performance.

2. Experimental

2.1. Materials and reagents

D-(+)-Glucose (purity > 99%) was purchased from J&K (Beijing, China). NaOH, HNO_3 (65%) and HCl (36–38%) were purchased from Jiangtian Chemical Technology Co., Ltd. (Tianjin, China). TC, $Bi(NO_3)_3{\cdot}5H_2O$, $Na_2WO_4{\cdot}4H_2O$, KI and $AgNO_3$ were obtained from Guangfu Technology Development Co., Ltd. Methanol and ethanol were purchased from Concord Technology Co., Ltd. Benzoquinone was purchased from Sigma Aldrich. All the chemicals were used without further purification.

2.2. Preparation of photocatalysts

2.2.1. Preparation of carbon dots (CDs)

CDs were synthesized by an alkali-assisted ultrasonic treatment modified from Kang's method [33]. In a typical experiment, 0.01 mol of glucose was dissolved in 10 mL of deionized water which was then added with 10 mL of NaOH solution (0.5 mol/L). The mixture was magnetically stirred for 30 min and subjected to an ultrasonic treatment (500 W, 40 kHz) for 4 h at room temperature. The solution was adjusted to pH 7 with HCl (36–38%) followed by dialysis (MWCO 1000) to remove any impurities. The solution was freeze-dried and brown powder was obtained, which was dissolved in 20 mL of deionized water. Thus, water-soluble CDs (0.18 g/L) were obtained.

2.2.2. Preparation of CDs-Bi_2WO_6

CDs-Bi_2WO_6 were synthesized by a facile hydrothermal method which was reported by Wang et al. [10]. Briefly, 10 mL sodium tungstate (Na_2WO_4) solution (0.05 mol/L) was added into 10 mL of bismuth nitrate ($Bi(NO_3)_3$) solution (0.1 mol/L)) with a certain amount of CDs solution added. The brown suspension was magnetically stirred for 30 min and ultrasonicated for 30 min. After adjusted to pH 1 using HNO_3 (1 mol/L), the suspension was transferred into a 40 mL Teflon-lined stainless steel autoclave and heated at 140 °C for 20 h in an oven. Subsequently, the autoclave was cooled down to room temperature. The yellowish products were collected by centrifugation at 8000 rpm, washed with deionized water and ethanol, and dried at 80 °C overnight. A pre-determined volume of CDs solution (corresponding to 0.5, 1.5, 2.5, 5 wt% CDs) was used for the synthesis. Preliminary experiments indicated that the composite synthesized by addition of 2.5 wt% CDs solution displayed the best photocatalytic activity (Fig. S2a). Thus, this condition was selected to synthesize the binary composite and the product was labeled as CDs2.5-Bi_2WO_6.

2.2.3. Preparation of Ag^+-CDs2.5-Bi_2WO_6

Ag^+-CDs2.5-Bi_2WO_6 were synthesized by a modified impregnation method [34]. An appropriate amount of $AgNO_3$ was dissolved in 10 mL of deionized water to form a clear solution (0.1 mol/L). 0.1 g of CDs2.5-Bi_2WO_6 was mixed with a certain volume of $AgNO_3$ solution based on Ag wt%. The suspension was subsequently stirred at room temperature for 1 h in dark (A preliminary experiment indicated that the adsorption of Ag^+ on the catalyst attained equilibrium at 30 min). Then the target product was obtained after drying the solvent under gentle nitrogen flow. The ternary photocatalysts obtained by adding appropriate $AgNO_3$ were defined as 0.5Ag^+-CDs2.5-Bi_2WO_6, 1Ag^+-CDs2.5-Bi_2WO_6, 5Ag^+-CDs2.5-Bi_2WO_6, 10Ag^+-CDs2.5-Bi_2WO_6, respectively.

To further understand the roles of Ag^+ and Ag on the photocatalytic activities, 5Ag^+-Bi_2WO_6 was prepared with Bi_2WO_6 as precursor following the same procedure stated as above. 5Ag-CDs2.5-Bi_2WO_6 was prepared by a photoreduction method, which was described in SI.

2.3. Characterization of the as-prepared materials

The morphologies and microstructures of the products were characterized by a field emission scanning electron microscopy (FESEM, LEO, 1530vp, Germany, with EDX analyzer), and a high-resolution transmission electron microscopy (HRTEM, JEM-2010FEF, Japan). Crystallographic information was obtained by an X-ray diffraction (XRD, D/MAX 2500 V diffractometer, Rigaku, Japan) with monochromatized Cu Kα radiation under 40 kV and 100 mA and the scanning range was from 10° to 80°. The X-ray photoelectron spectroscopy (XPS, Kratos Axis Ultra DLD) using monochromatized Al Kα X-ray as the excitation source was applied to study the composition and chemical state of the elements. The FT-IR spectra was carried out on MAGNA-560 Nicolet. Thermogravimetry (TG) was measured by thermogravimetric analyzer (NETZSCH TG209 Germany). The samples were subjected to a linear temperature ramp of 10.0 (K/min) in N_2 air. UV–vis diffuse reflectance spectra (DRS) of the samples were obtained on a Hitachi U-3010 spectrometer in the range of 200–800 nm. The photoluminescence (PL) spectra was recorded with an F-4500 fluorescence spectrophotometer.

Photoelectrochemical test was performed using an electrochemical analyzer (Chenhua Instruments Co., Shanghai) in a conventional three electrodes system with ITO/photocatalyst electrode serving as the working electrode, a platinum wire used as a counter electrode, saturated Ag/AgCl electrode used as a reference electrode. Na_2SO_4 solution (0.1 mol/L) was utilized as electrolyte in a single-compartment quartz cell. Xe lamp of 500 W was utilized as a visible light source with cutoff filter (λ > 400 nm). The photoresponses of the photocatalysts were measured at 0.0 V as visible light was switched on and off at certain intervals [9].

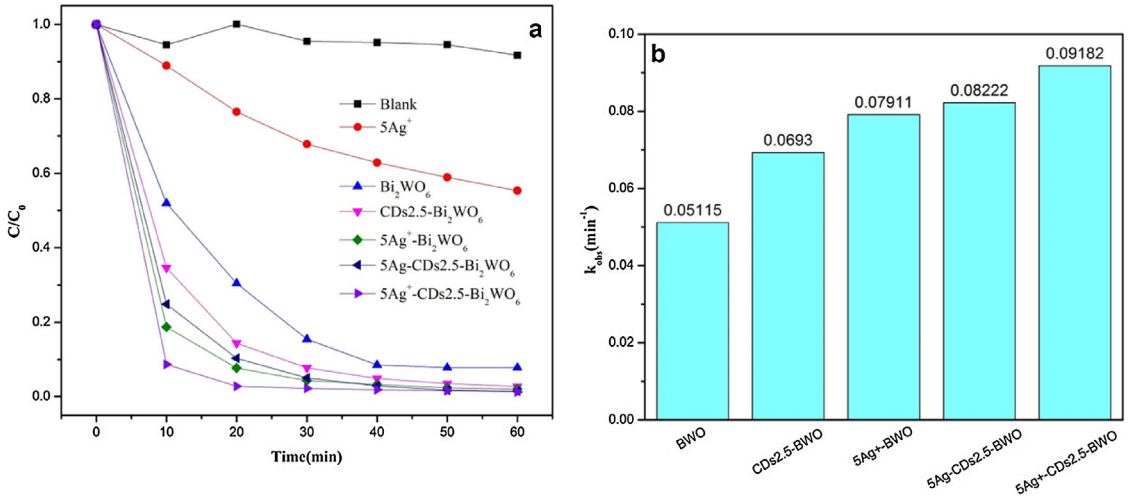

Fig. 1. Photocatalytic degradation of TC at 20 mg/L (a) and pseudo-first-order rate constant (k_{obs}) (b) with the as-prepared photocatalysts (Bi_2WO_6, CDs2.5-Bi_2WO_6, $5Ag^+$-Bi_2WO_6, 5Ag-CDs2.5-Bi_2WO_6, $5Ag^+$-CDs2.5-Bi_2WO_6, 0.5 g/L) and with only 5% Ag^+ in the solution under simulated solar-light irradiation.

2.4. Photocatalytic experiment and TC analysis

Photocatalytic experiments were conducted in an XPA-7 photochemical reactor (Xujiang Electromechanical plant, Nanjing, China). An 800 W Xe lamp without cutoff filter provided simulated solar-light irradiation. In a typical procedure, 20 mL of TC (20 mg/L) and 0.01 g of photocatalysts (0.5 g/L) were put in a 50 mL quartz tube. Before illumination, the suspension was constantly stirred for 30 min in dark until the adsorption-desorption equilibrium was established between TC and photocatalysts. At given intervals, 1 mL of an aliquot was sampled and centrifuged at 10,000 rpm. The supernatant was withdrawn for TC analysis.

TC in the supernatant was analyzed on a high performance liquid chromatography (HPLC, Agilent 1260 infinity, Agilent Corporation, USA) with a VWD detector (Wavelength at 355 nm) and the column was a Waters XTerra MS C18 (particle size 5 μm, 2.1 × 150 mm). The mobile phase consisted of 65% methanol and 35% water (with 0.167% phosphoric acid) at a flow rate of 0.15 mL/min. The total organic carbon (TOC) was measured by a TOC analyser (MultiN/C UV, Analytic Jena, Germany).

3. Results and discussion

3.1. Highly efficient photocatalytic degradation of TC with Ag^+-CDs-Bi_2WO_6

The photocatalytic degradation of TC by the as-prepared materials followed the pseudo-first-order reaction kinetic model:

$$-ln(C_t/C_0) = k_{obs}t$$

where C_0 and C_t are TC concentrations in aqueous phase (mg/L) at beginning and reaction time t. k_{obs} is the pseudo-first-order rate constant (min^{-1}) and t is reaction time (min).

The degradation kinetics and reaction rate constant of TC with as-prepared photocatalysts are shown in Fig. 1. TC was rarely degraded in the control test without photocatalysts, indicating it is resistant to photolysis in water under solar light irradiation. The CDs2.5-Bi_2WO_6 displayed better photoactivity (k_{obs} 0.06930, Fig. 1b) than pure Bi_2WO_6. In particular, $5Ag^+$-CDs2.5-Bi_2WO_6 displayed extremely high photocatalytic efficiency with a k_{obs} (0.09229, Fig. 1b). Nearly 92% TC was degraded in 10 min and almost fully removed in 20 min. Similar results could be observed from the UV–vis spectra in which the peak of TC almost disappeared after 20 min of reaction (Fig. S5a). The k_{obs} (0.09229) of $5Ag^+$-CDs2.5-Bi_2WO_6 was 1.3 fold of that using CDs2.5-Bi_2WO_6 and 1.8 fold of that using pure Bi_2WO_6. $5Ag^+$-Bi_2WO_6 (k_{obs} 0.07911) displayed better photoactivity than Bi_2WO_6 and CDs2.5-Bi_2WO_6, but still lower than $5Ag^+$-CDs2.5-Bi_2WO_6, suggesting that Ag^+ displayed an important role in enhancing the photoactivity and CDs was indispensable as well. Moreover, the photoactivity of 5Ag-CDs2.5-Bi_2WO_6 was apparently lower than that of $5Ag^+$-CDs2.5-Bi_2WO_6, which indicated the different mechanism of Ag^+ and Ag. Overall, $5Ag^+$-CDs2.5-Bi_2WO_6 displayed the highest activity among all these photocatalysts, implying that there were synergistic effects between CDs and Ag^+ in the Ag^+-CDs-Bi_2WO_6 system.

As shown in Fig. S2b, the photocatalytic activity increased gradually as the amount of Ag^+ in the solution increased. When the amount of Ag^+ further increased to 10 wt%, the photocatalytic activity reduced slightly, which could be due to that redundant Ag might act as a recombination center, or/and cover the active sites of Bi_2WO_6 [35]. It is worth noting that the color of the suspension containing Ag^+ gradually turned to brownish red in a few minutes after irradiation was initiated, suggesting that Ag^+ was reduced as Ag on the surface of Bi_2WO_6. Photoreduction was commonly used in preparation of Ag-based photocatalysts, which occurred

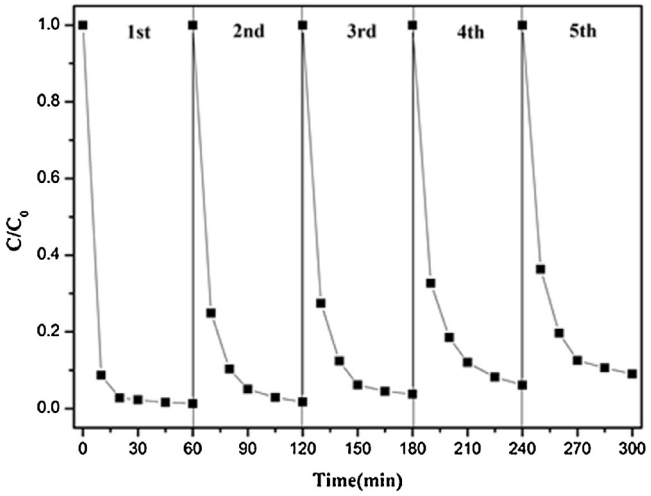

Fig. 2. Cycling test for the photocatalytic degradation of TC (20 mg/L) by $5Ag^+$-CDs2.5-Bi_2WO_6 (0.5 g/L).

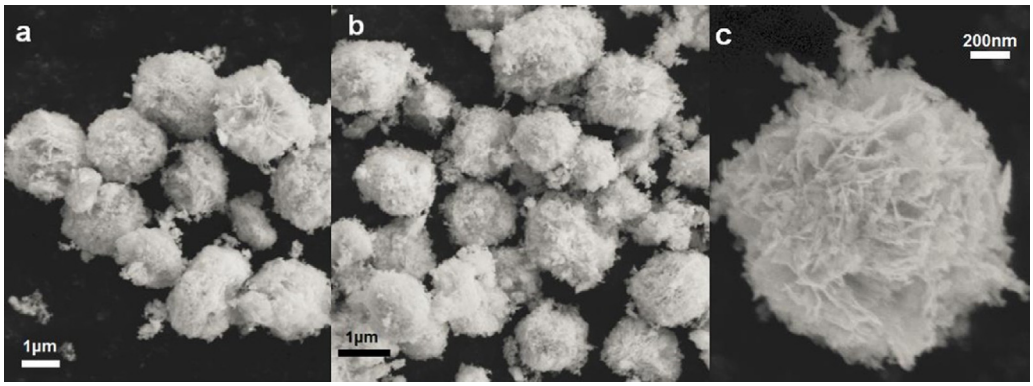

Fig. 3. FESEM images of the as-prepared photocatalysts. (a) CDs2.5-Bi_2WO_6; (b, c) R5Ag^+-CDs2.5-Bi_2WO_6.

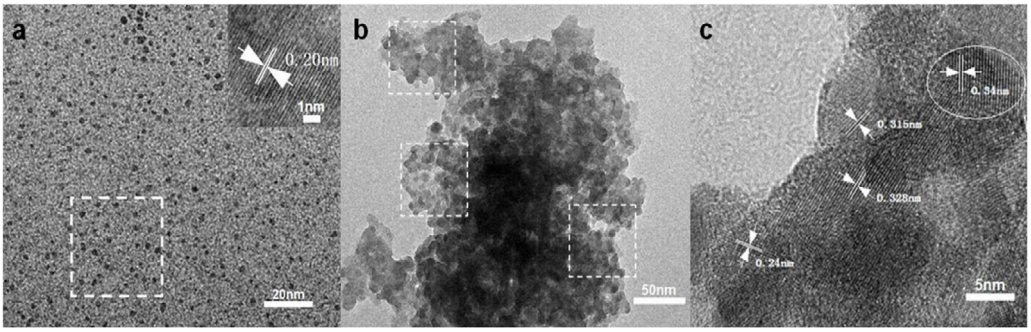

Fig. 4. HRTEM images of the as-prepared materials. (a) CDs (inset: high magnification of a CDs); (b, c) R5Ag^+-CDs2.5-Bi_2WO_6.

simultaneously with the process of photodegradation in the system [36]. When Ag^+ alone was added, the solution also became brownish red and a small portion of TC was removed [37]. This phenomenon indicated that Ag^+ itself made some contribution to the degradation of TC in the Ag^+-CDs-Bi_2WO_6 system (Fig. 1a).

For the Ag^+-CDs2.5-Bi_2WO_6 composite catalysts, they were recovered from the brownish red suspension after reaction and subjected for comprehensive characterization, which were discussed in the following section. The recovered ternary photocatalysts were named as RAg^+-CDs2.5-Bi_2WO_6 ("R" is the initial of "recovered". Here Ag^+ on the photocatalyst has been reduced to Ag). The images of all the as-prepared and recovered photocatalysts are shown in Fig. S1.

The total organic carbon (TOC) was determined and the results are presented in Table 1. After 90 min photoreaction, 64% of TOC was removed in the system of 5Ag^+-CDs2.5-Bi_2WO_6, which was much higher than that of pure Bi_2WO_6 (36%) and CDs2.5-Bi_2WO_6 (42%). In previous studies, $Ni_{0.4}Cu_{0.6}Fe_2O_4$ (dosage 1 g/L) and C-N-S/TiO_2 (dosage 0.5 g/L, same as our study) were used for TC degradation under solar-light irradiation [38,39], and TOC was removed 55% in 360 min and 74% in 180 min, respectively. Thus, 5Ag^+-CDs2.5-Bi_2WO_6 exhibited a very desirable mineralization capacity to TC.

Table 1
TOC analysis of TC (20 mg/L) degradation by Bi_2WO_6, CDs2.5-Bi_2WO_6, 5Ag^+-CDs2.5-Bi_2WO_6 (0.5 g/L) under simulated solar-light irradiation for different time periods.

Catalysts	TOC Removal (%)			
	Time			
	0 min	30 min	60 min	90 min
Bi_2WO_6	0%	32.53%	34.85%	36.31%
CDs2.5-Bi_2WO_6		37.43%	39.65%	41.91%
5Ag^+-CDs2.5-Bi_2WO_6		51.15%	57.42%	63.77%

Recycle test was conducted to investigate the stability and reusability of the as-prepared photocatalyst. After reaction, 5Ag^+-CDs2.5-Bi_2WO_6 was centrifuged and collected, then washed by deionized water and dried for the next run. As shown in Fig. 2, 5Ag^+-CDs2.5-Bi_2WO_6 still exhibit desirable photocatalytic performance, and about 91% of TC could be degraded in 60 min after four recycling runs. The photoactivity experienced a slightly loss after four recycling runs due to the mass loss during the process of collecting photocatalyst. In addition, the recovered R5Ag^+-CDs2.5-Bi_2WO_6 after the first cycle was converted to 5Ag-CDs2.5-Bi_2WO_6, which displayed poorer photoactivity than original ternary

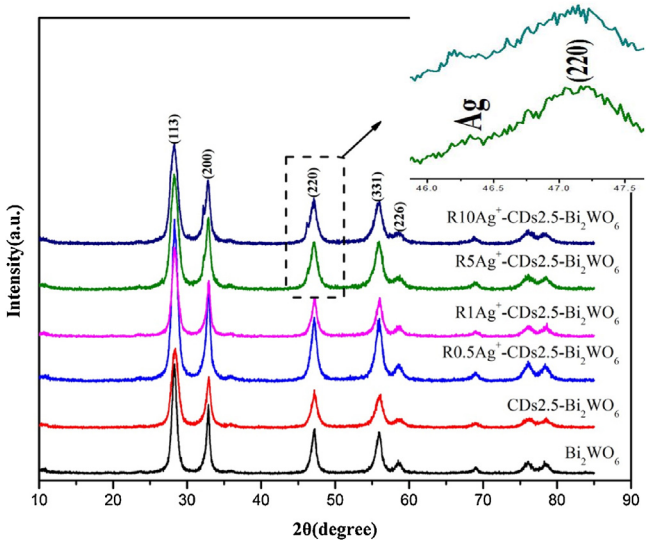

Fig. 5. XRD patterns of the as-prepared Bi_2WO_6, CDs2.5-Bi_2WO_6 and R0.5, 1, 5, 10Ag^+-CDs2.5-Bi_2WO_6; inset: enlarged images for specific refraction degrees.

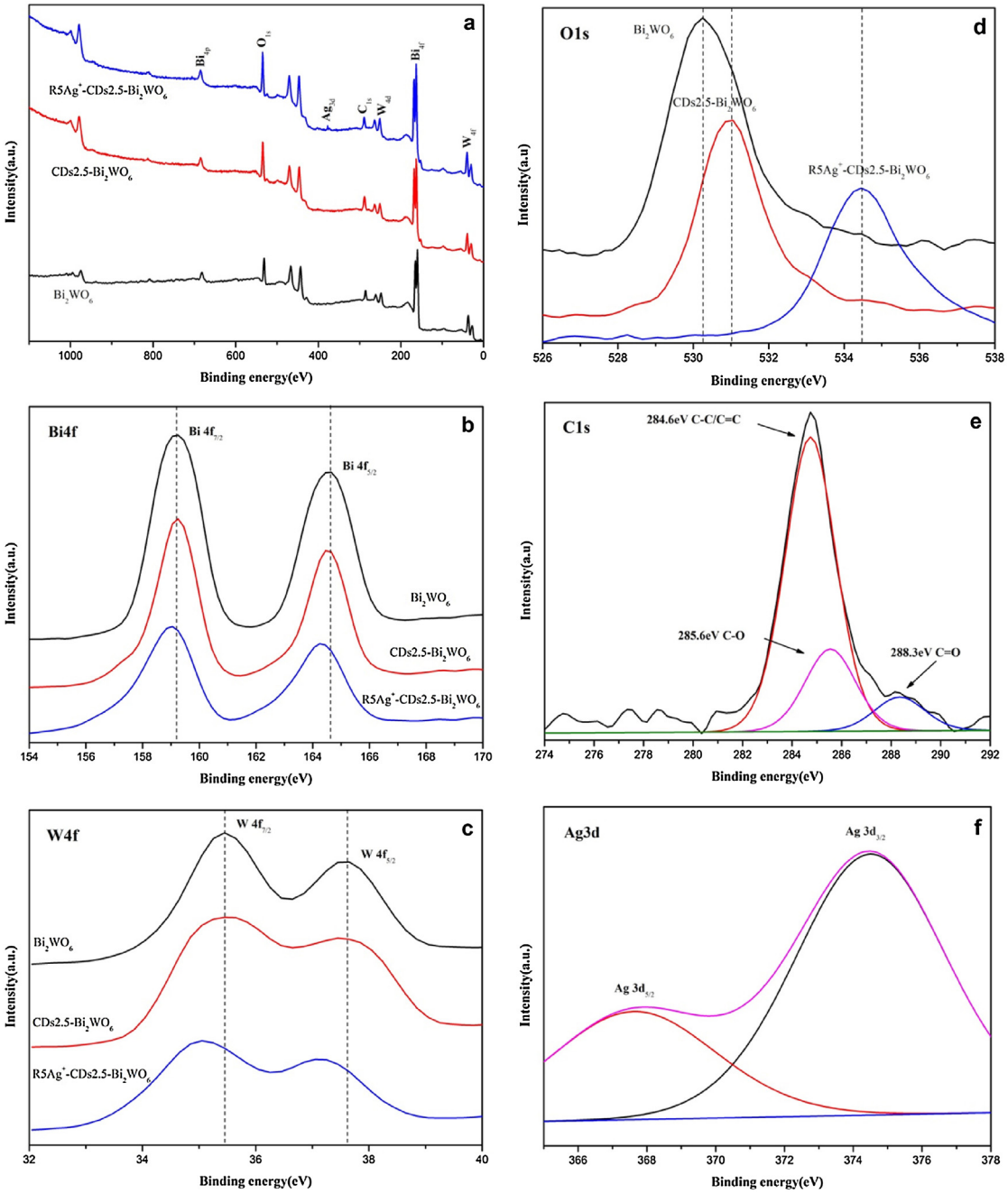

Fig. 6. XPS spectra of the as-prepared photocatalysts. (a) Full scan; (b, c) Bi 4f and W 4f; (d–f) O 1s, C1s, Ag 3d of R5Ag$^+$-CDs2.5-Bi_2WO_6.

photocatalysts. This may also contribute to the decreased photoactivity in the recycling tests. The results suggest that 5Ag$^+$-CDs2.5-Bi_2WO_6 kept its photocatalytic activity without distinct photocorrosion during the oxidation of pollutants.

3.2. Morphology and compositions of the as-prepared photocatalysts

The morphologies and microstructures of the as-prepared photocatalysts were characterized by FESEM (Fig. 3). R5Ag$^+$-CDs2.5-Bi_2WO_6 presented uniform microsphere structure with size of 0.5–2 μm in diameter (Fig. 3b). It mainly inherited the structure of CDs2.5-Bi_2WO_6 (Fig. 3a), indicating that no significant change occurred during the photoreduction of Ag$^+$. As shown in Fig. 3c, the microsphere was assembled by numerous Bi_2WO_6 nanosheets interlaced with each other. CDs and Ag were not obviously visible on the nanosheets due to their small size and low content. The EDX result in Fig. S6 shows the elemental compositions of R5Ag$^+$-CDs2.5-Bi_2WO_6. Apart from Bi, W, O, the signal of Ag was observed, indicating successful doping of Ag$^+$ and its conversion to Ag. The elements of C and Cu originated mainly from the FESEM grid. The content of the reduced Ag in the R5Ag$^+$-CDs2.5-Bi_2WO_6 was estimated to be about 3.6 wt%.

The morphologies of the as-prepared materials were further analyzed using HRTEM (Fig. 4). The black dots in Fig. 4a represent CDs, which were uniform and nearly spherical without aggregation. The inset of Fig. 4a confirmed the crystalline structure of CDs with lattice spacing of 0.20 nm, which was identified as the (102) diffraction plane of sp^2 graphitic carbon [40]. Based on the statistics of a designated area, a majority of CDs were in 1–4 nm, which was in

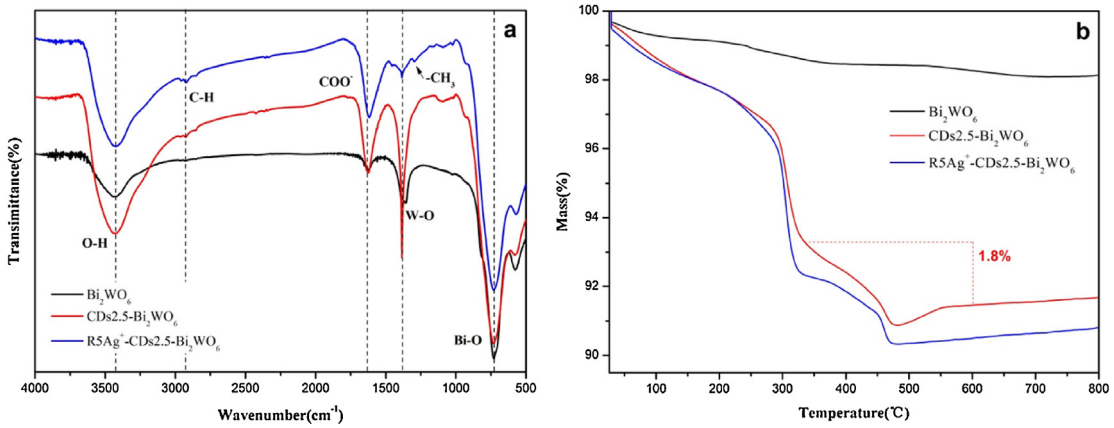

Fig. 7. (a) FT-IR spectra of the as-prepared Bi_2WO_6, CDs2.5-Bi_2WO_6 and R5Ag^+-CDs2.5-Bi_2WO_6; (b) TG curves of the as-prepared Bi_2WO_6, CDs2.5-Bi_2WO_6, and R5Ag^+-CDs2.5-Bi_2WO_6.

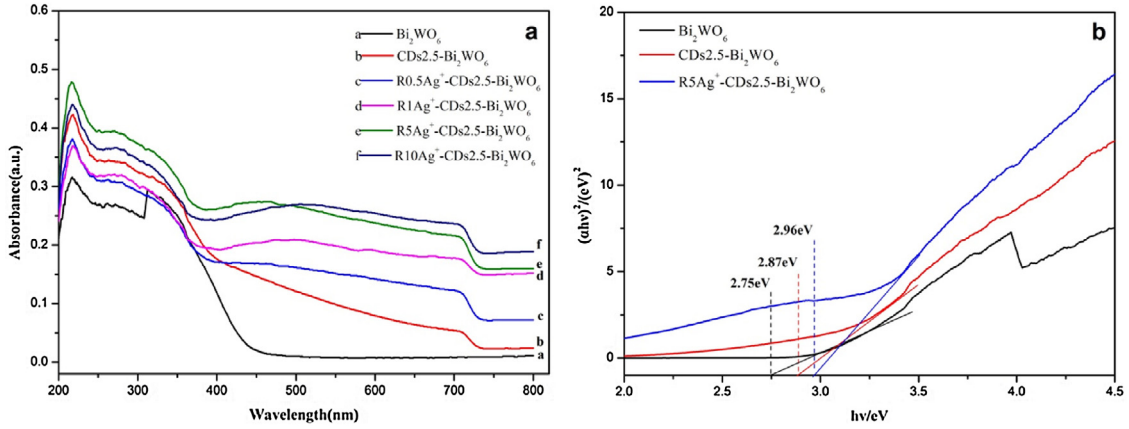

Fig. 8. (a) UV–vis diffuse reflectance spectra of the as-prepared Bi_2WO_6, CDs2.5-Bi_2WO_6, and R0.5, 1, 5, 10Ag^+-CDs2.5-Bi_2WO_6. (b) Using Tauc plot to calculate the band gaps of the as-prepared photocatalysts.

accordance of quantum dots (Fig. S3a). The UV–vis absorption spectrum in Fig. S3b further supports the formation of CDs. A distinct peak around 270–280 nm refers to n-π^* transition of the C—O band [41,42]. Fig. 4b shows the sphere-like structure of R5Ag^+-CDs2.5-Bi_2WO_6, supporting the results of FESEM. Large numbers of small dots less than 10 nm were uniformly distributed on the surface of the nanosheets, which might be a strong evidence for successful co-doping of CDs and Ag. Fig. 4c reveals the lattice spacing of R5Ag^+-CDs2.5-Bi_2WO_6. The lattice spacing at 0.315 and 0.328 nm was due to the (113) and (131) planes of Bi_2WO_6 [43,44]. The lattice spacing at 0.34 nm was characteristic of the (112) facet of graphitic carbon in CDs [45]. Another lattice spacing of 0.24 nm corresponded to the crystal plane for Ag (111) facet [46]. These results support that CDs and Ag were successfully attached on the surface of Bi_2WO_6.

The X-ray diffraction (XRD) patterns of the as-prepared and collected photocatalysts are recorded in Fig. 5. All the distinct diffraction peaks were perfectly indexed to pure orthorhombic structure Bi_2WO_6 (JCPDS Card No. 39-0256) [47], suggesting the incorporated CDs and Ag did not significantly change the structure of Bi_2WO_6. The peaks at 28.3° and 56°, corresponding to (113) and (131) planes of Bi_2WO_6, agreed well with the results of HRTEM. The characteristic peak of carbon at 26° was too weak to be observed due to the low amount of CDs [48]. In addition, the (131) diffraction peak of Bi_2WO_6 might overlap with the characteristic peak at 26° [49]. As the amount of Ag^+ in RAg^+-CDs2.5-Bi_2WO_6 increased over 5%, a small peak appeared at about 46°, corresponding to Ag plane [50], indicating that Ag was successfully doped during the reaction.

XPS analysis was carried to investigate the surface elemental compositions and chemical states, as shown in Fig. 6. The binding energies were calibrated using C_{1s} peak of aliphatic carbon at 284.6 eV. Fig. 6a provides the full scan of XPS spectra in a wide energy range. The XPS peak of C1s in pure Bi_2WO_6 was due to the adventitious hydrocarbon from the XPS instrument itself [51]. The intensity of C1s peak markedly increased in the samples containing CDs. Ag was found in the R5Ag^+-CDs2.5-Bi_2WO_6 in addition to Bi, W, O and C elements (Fig. 6a). The spectra of Ag 3d (Fig. 6f) could be fitted into two parts, 368.4 (Ag $3d_{3/2}$) and 374.4 eV (Ag $3d_{5/2}$) [24]. Fig. 6(b,c) are the high-resolution XPS spectra of Bi 4f and W 4f. The peaks at 159.1 and 164.4 eV were attributed to Bi $4f_{7/2}$ and Bi $4f_{5/2}$ of Bi^{3+} in Bi_2WO_6 while those at 35.4 and 37.5 eV were attributed to W $4f_{5/2}$ and W $4f_{7/2}$. Doping Bi_2WO_6 with CDs slightly affected the binding energy of Bi 4f (Fig. 6b), but dramatically affected the shape of W 4f peaks. The two peaks of W 4f were slightly merged and could not be separated (Fig. 6c). This suggested that the chemical environment surrounding W changed significantly as the CDs were attached on Bi_2WO_6 [36]. With the deposition of Ag on the surface of CDs2.5-Bi_2WO_6, the XPS peaks of Bi 4f and W 4f experienced a slight shift to lower binding energy due to the chemical interaction between Ag and CDs2.5-Bi_2WO_6 [52]. Similar results are also observed for O 1s (Fig. 6d). The peak at 530.3 eV assigned to the lattice oxygen shifted toward higher binding energies [53], with 0.7 eV for CDs2.5-Bi_2WO_6 and 3.1 eV for R5Ag^+-CDs2.5-Bi_2WO_6. The relatively large peak shift in the recovered R5Ag^+-CDs2.5-Bi_2WO_6 may be due to the combined effects of the heterojuction structure

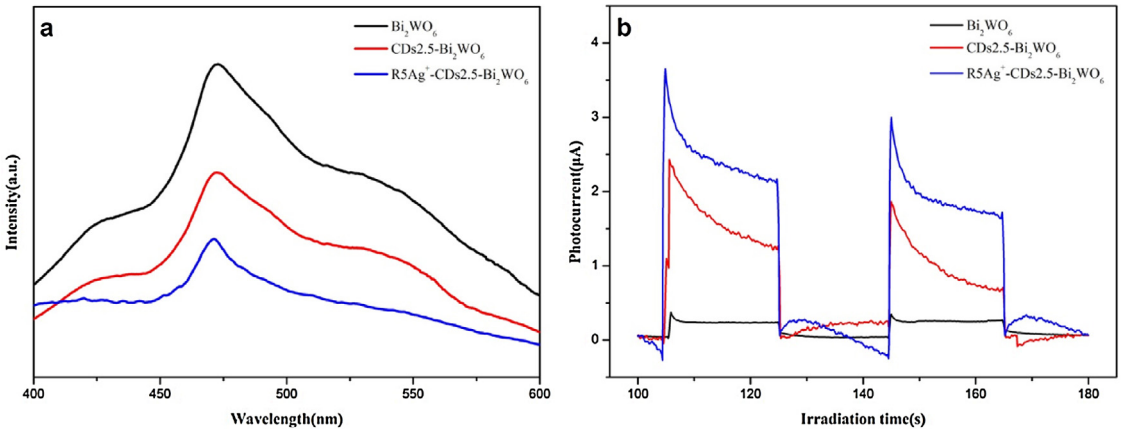

Fig. 9. (a) PL spectra of the as-prepared Bi_2WO_6, CDs2.5-Bi_2WO_6, and R5Ag^+-CDs2.5-Bi_2WO_6; (b) photocurrent curves of as prepared Bi_2WO_6, CDs2.5-Bi_2WO_6 and R5Ag^+-CDs2.5-Bi_2WO_6.

formed in the composite and the functional groups of degradation products attached to the R5Ag^+-CDs2.5-Bi_2WO_6 [54–58]. The C1s band splitted into three parts (Fig. 6e). The main peak at 284.6 eV in the C1s spectra could be assigned to C—C (sp^2-hybridized graphite carbon)/C=C bond, the binding energy at 285.6 and 288.3 eV could be ascribed to C—O and C=O bond respectively [59]. These three peaks indicated the presence of CDs in CDs2.5-Bi_2WO_6. XPS results further demonstrated the coexistence of Ag and CDs, and there was a chemical rather than physical interactions between CDs, Ag and Bi_2WO_6. The successful incorporation would favor the transfer of electrons among CDs, Ag and Bi_2WO_6 [47].

The FT-IR is illustrated in Fig. 7a. The stretching vibrations of O—H and C—H at 3430 cm^{-1} and 2960 cm^{-1} were observed. The main absorption bands at 400–1700 cm^{-1} were ascribed to Bi—O stretching mode and W—O—W bridge stretching model [60]. For CDs2.5-Bi_2WO_6, the new peak at 1618 cm^{-1} was related to O—C—O asymmetric vibrations, supporting that CDs were successfully attached to Bi_2WO_6 [61]. There is also a small peak at 1618 cm^{-1} for Bi_2WO_6, which might be attributed to the adsorbed surface water at around 1630–1650 cm^{-1} [62]. For R5Ag^+-CDs2.5-Bi_2WO_6, apart from the peak of O—C—O, another tiny peak assigned to $-CH_3$ at around 1300 cm^{-1} might be the signal of residual TC [63] or intermediate products absorbed on the collected photocatalyst.

The TG curves are shown in Fig. 7b. The mass loss from 200 to 300 °C originated from water adsorbed on its surface [64]. For CDs2.5-Bi_2WO_6, the TG curve could be divided into two apparent steps with a 8.8 wt% total weight loss. The first loss at 200–320 °C was due to the release of bound water and surface hydroxylated species. The second loss at 320–600 °C, corresponding to 1.8 wt% weight loss, was due to the slow combustion of carbon in the CDs [65]. This result was closely in line with the study of Di et al. [66], which demonstrated that 2% was the optimal dosage of carbon quantum dot. The extra 1% total weight loss on TG curve of R5Ag^+-CDs2.5-Bi_2WO_6 was probably due to the absorbed intermediates or degradation products of TC, which verified the FT-IR result.

3.3. *Mechanisms for the enhanced photocatalytic performance of 5Ag^+-CDs2.5-Bi_2WO_6*

Fig. 8a illustrates the UV–vis diffuse reflectance spectra of the as-prepared catalysts. The light harvesting capacities of the binary (CDs2.5-Bi_2WO_6) and ternary catalysts (R0.5, 1, 5, 10Ag^+-CDs2.5-Bi_2WO_6) were significantly enhanced in the visible-light region compared to pure Bi_2WO_6. A distinct red shift was observed as CDs was doped on Bi_2WO_6. The intrinsic property of CDs, together with the interaction between CDs and Bi_2WO_6, gave rise to the enhancement of visible-light photoresponse [67]. The photoabsorption ability was further strengthened as the amount of Ag^+ increased, with a broad and intense absorption band from 400 to 800 nm. This phenomenon might be attributed to the localized surface plasmon resonance (SPR) effect of the reduced plasmonic-Ag, leading to a wide band absorption around 400 nm [24]. The surface plasmon absorption in the Ag nanoparticles arises from the collective oscillations of the free conduction band electrons that are enhanced by the incident electromagnetic proportion of irradiation [26]. The SPR effect makes Ag absorb more visible light, promoting the utilization of the visible-light's energy for photocatalysts.

For a crystalline semiconductor, the optical band gap can be calculated by Tauc approach. The detailed calculation process is presented in the Supporting information. The band gap of Bi_2WO_6, CDs2.5-Bi_2WO_6, R5Ag^+-CDs2.5-Bi_2WO_6 were determined as 2.75, 2.87, 2.96 eV, respectively (Fig. 8b), with corresponding energy band structure parameters listed in Table S1.

Fig. 9a shows the photoluminescence (PL) spectra of the as-prepared catalysts at an excitation wavelength of 325 nm. The emission band located at 480–500 nm. The PL intensity of CDs2.5-Bi_2WO_6 was slightly lower than that of Bi_2WO_6. However, a sharp decrease was observed for R5Ag^+-CDs2.5-Bi_2WO_6. This was the result of enhanced charge separation and efficient charge

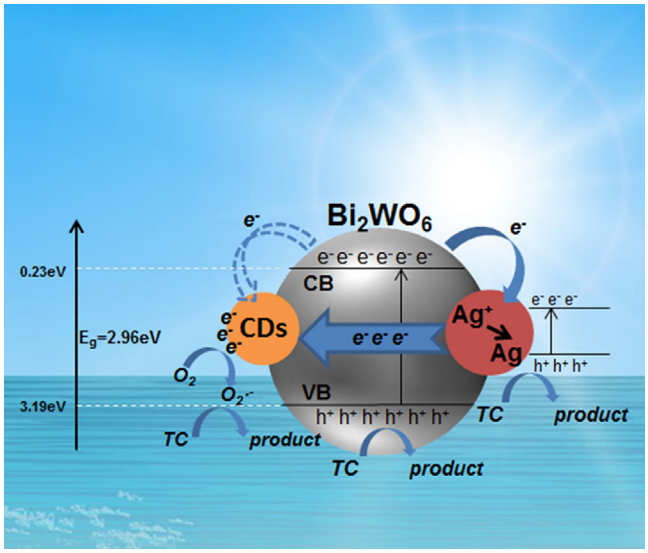

Fig. 10. Schematic diagram of the charge transfer in the 5Ag^+-CDs2.5-Bi_2WO_6 combined with the possible reaction mechanisms of photocatalysis under solar light.

transfer among CDs, Ag and Bi_2WO_6 [68]. The transient photocurrent response curves were also measured and the results are shown in Fig. 9b. Compared with pure Bi_2WO_6, CDs2.5-Bi_2WO_6 exhibited fast and reproducible transient photocurrent responses under several on–off cycles of intermittent visible-light irradiation. R5Ag^+-CDs2.5-Bi_2WO_6 presented the strongest transient photocurrent response which was about 1.5 times higher than that of CDs2.5-Bi_2WO_6. This result further supported that doping of CDs and Ag promoted transfer of the photogenerated charges and inhibited their rapid recombination [69].

Effects of different scavengers on degradation of TC by 5Ag-CDs2.5-Bi_2WO_6 are shown in Fig. S5b. Only when KI or benzoquinone was added in the system, the photocatalytic activity dramatically decreased. This indicates that holes and superoxide species were the main active species for the reaction system.

The diagram in Fig. 10 illustrates the photocatalytic mechanisms. As solar light irradiated on 5Ag^+-CDs2.5-Bi_2WO_6, electrons (e^-) on the valence band (VB) of Bi_2WO_6 were produced and transferred to the conduction band (CB), leaving holes (h^+) in the VB. At this time, CDs mainly acted as electron acceptors to trap a portion of electrons excited from Bi_2WO_6, thus hindering the recombination of electron-hole pairs [70].

Meanwhile, Ag^+ not only trap electrons excited from Bi_2WO_6, but also trap electrons to oxidize TC under irradiation. As Ag^+ was photoreduced to Ag and deposited on CDs2.5-Bi_2WO_6 gradually, a new heterojunction structure of Ag-CDs-Bi_2WO_6 was formed. It was reported that Ag supplied a fast lane for charge transfer and its surface acted as a charge-trap center to host more active sites for photocatalytic degradation [71]. Under solar light irradiation, plasmon-induced electron-hole pairs were formed on the surface of Ag due to the SPR effect. The photo-generated electrons excited from Bi_2WO_6 were entrapped by Ag to recombine with some of the plasmon-induced holes produced by Ag due to its high Schottky barrier at the metal/semiconductor interface [46]. The remained electrons on Ag continued transferring to CDs so that the charge transfer efficiency was further improved [72]. The sequence of electron transfer is judged by the difference of work function. The work function of Ag is about 4.2 eV. The featured graphitic-carbon structure and oxygen-containing groups of CDs is considered as quantum-sized graphene oxide (GO), with a work function of 4.7-5.2 eV [73–75]. Electrons tend to move to materials with higher work function [76]. Consequently, it was speculated that electrons preferably transferred to Ag at first, subsequently to CDs as an ultimate reservoir. Once electrons reached CDs, they reacted with oxygen in the solution to yield $O_2^{\bullet -}$. Holes are reluctant to react with OH^- or H_2O to form $^\bullet OH$ radicals, because the standard redox potential of the valence band is more negative than that of $OH^-/^\bullet OH$ [77]. Therefore, h^+ (Ag & Bi_2WO_6) and $O_2^{\bullet -}$ (CDs) were primary oxidant agents responsible for degrading TC molecules into intermediates and inorganic compounds.

As a result, the synergistic effects of CDs and Ag^+ gave rise to the highest photoactivity of 5Ag^+-CDs2.5-Bi_2WO_6 in the respects of electron transfer and visible light use.

4. Conclusions

A novel Ag^+-CDs-Bi_2WO_6 was successfully synthesized for the first time and the synergistic effects of Ag^+ and CDs were analyzed and discussed. CDs were evenly distributed on Bi_2WO_6 nanosheets and mainly worked as electron acceptors. Ag^+ in the solution could also trap electrons excited from the catalysts and TC under irradiation, and was subsequently converted to plasmonic Ag as a dopant. Due to the coexistence of CDs and Ag^+, the separation of the photogenerated electron-hole pairs and the use of visible light were distinctly improved, facilitating the photocatalytic degradation. 5Ag^+-CDs2.5-Bi_2WO_6 (0.5 g/L) exhibited the best photocatalytic activity as well as the degree of mineralization towards TC (20 mg/L). The recycled 5Ag^+-CDs2.5-Bi_2WO_6 displayed excellent stability and reusability. Photogenerated holes and superoxide radicals were the main active species responsible for the photocatalytic degradation.

Acknowledgements

The authors gratefully acknowledge the financial support of Ministry of Science and Technology (2014CB932001, 2012ZX07529-003), Tianjin Municipal Science and Technology Commission (13JCZDJC35900), and the Ministry of Education innovation team (IRT 13024).

Appendix A. Supplementary data

Supplementary data associated with this article can be found, in the online version, at http://dx.doi.org/10.1016/j.apcatb.2016.03.045.

References

[1] S.P. Kim, P. Eichhorn, J.N. Jensen, A.S. Weber, D.S. Aga, Environ. Sci. Technol. 39 (2005) 5816–5823.
[2] L. Zhang, X.Y. Song, X.Y. Liu, L.J. Yang, F. Pan, J.N. Lv, Chem. Eng. J. 178 (2011) 26–33.
[3] L.N. Shao, Z.M. Ren, G.S. Zhang, L.L. Chen, Mater. Chem. Phys. 135 (2012) 16–24.
[4] J. Jeong, W.H. Song, W.J. Cooper, J.Y. Jung, J. Greaves, Chemosphere 78 (2010) 533–540.
[5] Y.J. Wang, X.D. Zhu, R.J. Sun, D.M. Zhou, Chemosphere 92 (2013) 925–932.
[6] D.S. Bhatkhande, V.G. Pangarkar, A.A. Beenackers, J. Chem. Technol. Biotechnol. 77 (2001) 102–116.
[7] M.N. Chong, B. Jin, Christopher W.K. Chow, C. Saint, Water Res. 44 (2010) 2997–3027.
[8] D. Chatterjee, S. Dasgupta, J. Photochem. Photobiol. C: Photochem. Rev. 6 (2005) 186–205.
[9] C. Chang, L.Y. Zhu, S.F. Wang, X.L. Chu, L.F. Yue, ACS Appl. Mater. Interfaces 6 (2014) 5083–5093.
[10] C.Y. Wang, H. Zhang, F. Li, L.Y. Zhu, Environ. Sci. Technol. 44 (2010) 6843–6848.
[11] T. Saison, P. Gras, N. Chemin, C. Chaneíac, O. Durupthy, V. Brezova, C. Colbeau-Justin, J.P. Jolivet, J. Phys. Chem. C 117 (2013) 22656–22666.
[12] L.S. Zhang, H.L. Wang, Z.G. Chen, P.K. Wong, J.S. Liu, Appl. Catal. B: Environ. 106 (2011) 1–13.
[13] L. Ge, C.C. Han, J. Liu, Appl. Catal. B: Environ. 108–109 (2011) 100–107.
[14] S.L. Hu, R.X. Tian, Y.G. Dong, J.L. Yang, J. Liu, Q. Chang, Nanoscale 5 (2013) 11665–11671.
[15] H.T. Li, R.H. Liu, S.Y. Lian, Y. Liu, H. Huang, Z.H. Kang, Nanoscale 5 (2013) 3289–3297.
[16] F. Wang, Y.L. Zhang, Y. Liu, X.F. Wang, M.R. Shen, S.T. Lee, Z.H. Kang, Nanoscale 5 (2013) 1831–1835.
[17] S.Y. Lim, W. Shen, Z.Q. Gao, Chem. Soc. Rev. 44 (2015) 362–381.
[18] R.H. Liu, H. Huang, H.T. Li, Y. Liu, J. Zhong, Y.Y. Li, S. Zhang, Z.H. Kang, ACS Catal. 4 (2014) 328–336.
[19] X.J. Yu, J.J. Liu, Y.C. Yu, S.L. Zuo, B.S. Li, Carbon 68 (2014) 718–724.
[20] Y. Li, B.P. Zhang, J.X. Zhao, Z.H. Ge, X.K. Zhao, L. Zou, Appl. Surf. Sci. 279 (2013) 367–373.
[21] B.Y. Yu, S.Y. Kwak, J. Mater. Chem. 22 (2012) 8345–8353.
[22] H.J. Feng, M.H. Zhang, L.Y.E. Yu, Appl. Catal. A: Gen. 413–414 (2012) 238–244.
[23] S. Higashimoto, R. Shirai, Y. Osano, M. Azuma, H. Ohue, Y. Sakata, H. Kobayashi, J. Catal. 311 (2014) 137–143.
[24] E.P. Melián, O.G. Díaz, J.M.D. Rodríguez, G. Colón, J.A. Navío, M. Macías, J.P. Peña, Appl. Catal. B: Environ. 127 (2012) 112–120.
[25] S.Y. Zhu, S.J. Liang, Q. Gu, L.Y. Xie, J.X. Wang, Z.X. Ding, P. Liu, Appl. Catal. B: Environ. 119–120 (2012) 146–155.
[26] D.J. Wang, G.L. Xue, Y.Z. Zhen, F. Fu, D.S. Li, J. Mater. Chem. 22 (2012) 4751–4758.
[27] Q.S. Wu, Y. Cui, L.M. Yang, G.Y. Zhang, D.Z. Gao, Sep. Purif. Technol. 142 (2015) 168–175.
[28] H.W. Huang, K. Liu, K. Chen, Y.L. Zhang, Y.H. Zhang, S.C. Wang, J. Phys. Chem. C 118 (2014) 14379–14387.
[29] H.W. Huang, X. Han, X.W. Li, S.C. Wang, P.K. Chu, Y.H. Zhang, ACS Appl. Mater. Interfaces 7 (2015) 482–492.
[30] S. Obregón, G. Colón, Appl. Catal. B: Environ. 140–141 (2013) 299–305.
[31] M.S. Zhu, P.L. Chen, M.H. Liu, Langmuir 29 (2013) 9259–9268.
[32] H.X. Shi, J.Y. Chen, G.Y. Li, X. Nie, H.J. Zhao, P.K. Wong, T.C. An, ACS Appl. Mater. Interfaces 5 (2013) 6959–6967.

[33] Z. Ma, H. Ming, H. Huang, Y. Liu, Z.H. Kang, New J. Chem. 36 (2012) 861–864.
[34] Q.S. Wu, Y. Cui, L.M. Yang, G.Y. Zhang, D.Z. Gao, Sep. Purif. Technol. 142 (2015) 168–175.
[35] X.J. Bai, R.L. Zong, C.X. Li, D. Liu, Y.F. Liu, Y.F. Zhu, Appl. Catal. B: Environ. 147 (2014) 82–91.
[36] P. Wang, B.B. Huang, Y. Dai, M.H. Whangbo, Phys. Chem. Chem. Phys. 14 (2012) 9813–9825.
[37] Y.Y. Chen, Y.B. Xie, J. Yang, H.B. Cao, Y. Zhang, J. Environ. Sci. 26 (2014) 662–672.
[38] P.H. Wang, P.S. Yap, T.T. Lim, Appl. Catal. A: Gen. 399 (2011) 252–261.
[39] Y.Z. Hong, A. Ren, Y.H. Jiang, J.H. He, L.S. Xiao, W.D. Shi, Ceram. Int. 41 (2015) 1477–1486.
[40] S. Sahu, B. Behera, T.K. Maitib, S. Mohapatra, Chem. Commun. 48 (2012) 8835–8837.
[41] S.Y. Gao, Y.L. Chen, H. Fan, X.J. Wei, C.G. Hu, L.X. Wang, L.T. Qu, J. Mater. Chem. 2 (2014) 6320–6325.
[42] B.D. Yin, J.H. Deng, X. Peng, Q. Long, J.N. Zhao, Q.J. Lu, Q. Chen, H.T. Li, H. Tang, Y.Y. Zhang, S.Z. Yao, Analyst 138 (2013) 6551–6557.
[43] D.K. Ma, S.M. Huang, W.X. Chen, S.W. Hu, F.F. Shi, K.L. Fan, J. Phys. Chem. 113 (2009) 4369–4374.
[44] Y. Fu, C. Chang, P. Chen, X.L. Chu, L.Y. Zhu, J. Hazard. Mater. 244–245 (2013) 185–192.
[45] W. Kwon, S.W. Rhee, Chem. Commun. 48 (2012) 5256–5258.
[46] Y.H. Liang, S.L. Lin, L. Liu, J.S. Hu, W.Q. Cui, Appl. Catal. B: Environ. 164 (2015) 192–203.
[47] M.S. Gui, W.D. Zhang, Nanotechnology 22 (2011), 265601.
[48] D. Tang, H.C. Zhang, H. Huang, R.H. Liu, Y.Z. Han, Y. Liu, C.Y. Tong, Z.H. Kang, Dalton Trans. 42 (2013) 6285–6289.
[49] L.F. Yue, S.F. Wang, G.Q. Shan, W. Wu, L.W. Qiang, L.Y. Zhu, Appl. Catal. B: Environ. 176–177 (2015) 11–19.
[50] J. Ren, W.Z. Wang, S.M. Sun, L. Zhang, J. Chang, Appl. Catal. B: Environ. 92 (2009) 50–55.
[51] H.G. Yu, R. Liu, X.F. Wang, P. Wang, J.G. Yu, Appl. Catal. B: Environ. 111–112 (2012) 326–333.
[52] Y. Xue, X.T. Wang, Int. J. Hydrogen Energy 40 (2015) 5878–5888.
[53] F. Duan, Y. Zheng, M.Q. Chen, Appl. Surf. Sci. 257 (2011) 1972–1978.
[54] C. Chang, L.Y. Zhu, Y. Fu, X.L. Chu, Chem. Eng. J. 233 (2013) 305–314.
[55] J. Kang, H.J. Liu, Y.M. Zheng, J.H. Qu, J.P. Chen, J. Colloid Interface Sci. 344 (2010) 117–125.
[56] L. Wang, A.Q. Wang, Bioresour. Technol. 99 (2008) 1403–1408.
[57] S. Cherian, C.C. Warmser, J. Phys. Chem. B 104 (2000) 3624–3629.
[58] Q. Wang, C.C. Chen, D. Zhao, W.H. Ma, J.C. Zhao, Langmuir 24 (14) (2008) 7338–7345.
[59] J. Wang, Y.H. Ng, Y.F. Lim, G.W. Ho, RSC Adv. 4 (2014) 44117–44123.
[60] G.K. Zhang, F. Lv, M. Li, J.L. Yang, X.Y. Zhang, B.B. Huang, J. Phys. Chem. Solids 71 (2010) 579–582.
[61] H. Yu, H.C. Zhang, H. Huang, Y. Liu, H.T. Li, H. Ming, Z.H. Kang, New J. Chem. 36 (2012) 1031–1035.
[62] B. Long, Y.C. Huang, H.B. Li, F.Y. Zhao, Z.B. Rui, Z.L. Liu, Y.X. Tong, H.B. Ji, Ind. Eng. Chem. Res. 54 (2015) 12788–12794.
[63] M.E. Parolo, M.J. Avena, G. Pettinari, I. Zajonkovsky, J.M. Valles, M.T. Baschini, Appl. Clay Sci. 49 (2010) 194–199.
[64] Y.J. Wang, X.J. Bai, C.S. Pan, J. He, Y.F. Zhu, J. Mater. Chem. 22 (2012) 11568–11573.
[65] F.Y. Zheng, Z.H. Wang, J. Chen, S.X. Li, RSC Adv. 4 (2014) 30605–30609.
[66] J. Di, J.X. Xia, Y.P. Ge, H.P. Li, H.Y. Ji, H. Xu, Q. Zhang, H.M. Li, M.N. Li, Appl. Catal. B: Environ. 168–169 (2015) 51–61.
[67] H.P. Li, Y.H. Zhu, H.M. Cao, X.L. Yang, C.Z. Li, Mater. Res. Bull. 48 (2013) 232–237.
[68] Q. Xiao, J. Zhang, C. Xiao, X.K. Tan, Catal. Commun. 9 (2008) 1247–1253.
[69] S.L. Lin, L. Liu, J.S. Hu, Y.H. Liang, W.Q. Cui, Appl. Surf. Sci. 324 (2015) 20–29.
[70] H.C. Zhang, H. Huang, H. Ming, H.T. Li, L.L. Zhang, Y. Liu, Z.H. Kang, J. Mater. Chem. 22 (2012) 10501–10506.
[71] X.M. Zhang, Y.L. Chen, R.S. Liu, D.P. Tsai, Rep. Prog. Phys. 76 (2013) 046401.
[72] Y.G. Xu, H. Xu, J. Yan, H.M. Li, L.Y. Huang, Q. Zhang, C.J. Huang, H.L. Wan, Phys. Chem. Chem. Phys. 15 (2013) 5281–5830.
[73] N.T. Khoa, S.W. Kim, D.H. Yoo, E.J. Kim, S.H. Hahn, Appl. Catal. A: Gen. 469 (2014) 159–164.
[74] Z.L. Wang, J.H. Song, Science 312 (2006) 242–246.
[75] X. Jiang, J. Nisar, B. Pathak, J.J. Zhao, R. Ahuja, J. Catal. 299 (2013) 204–209.
[76] M.S. Zhu, P.L. Chen, M.H. Liu, J. Mater. Chem. 22 (2012) 21487–21494.
[77] J.Q. Lin, Z.Y. Guo, Z.F. Zhu, Ceram. Int. 40 (2014).

Update

Applied Catalysis B: Environmental
Volume 194, Issue , 5 October 2016, Page 61

DOI: https://doi.org/10.1016/j.apcatb.2016.04.041

Applied Catalysis B: Environmental 194 (2016) 61

Contents lists available at ScienceDirect

Applied Catalysis B: Environmental

journal homepage: www.elsevier.com/locate/apcatb

Corrigendum

Corrigendum to "Highly efficient photocatalysis toward tetracycline under simulated solar-light by Ag^{+}-CDs-Bi_2WO_6: Synergistic effects of silver ions and carbon dots" [Appl. Catal. B: Environ. 192 (2016) 277–285]

Zhuo Li, Lingyan Zhu*, Wei Wu, Shanfeng Wang, Liwen Qiang

Key Laboratory of Pollution Processes and Environmental Criteria, Ministry of Education, Tianjin Key Laboratory of Environmental Remediation and Pollution Control, College of Environmental Science and Engineering, Nankai University, Tianjin 300071, PR China

The authors regret to inform that the following corrections should be made in the respect to Acknowledgment.

The authors gratefully acknowledge the financial support of National Science Foundation (NSFC 21325730), Ministry of Science and Technology (2014CB932001, 2012ZX07529-003), Tianjin Municipal Science and Technology Commission (15JCZDJC40700), and the Ministry of Education innovation team (IRT 13024).

Author would like to apologize for the inconvenience caused.

DOI of original article: http://dx.doi.org/10.1016/j.apcatb.2016.03.045.

* Corresponding author at: The College of Environmental Science and Engineering, Nankai University, Tongyan Road 38, Tianjin 300350, PR China.
E-mail address: zhuly@nankai.edu.cn (L. Zhu).

http://dx.doi.org/10.1016/j.apcatb.2016.04.041